NEOPLASIA
www.neoplasia.com

Volume 10 Number 12 December 2008 pp. 1470–1480 **1470**

WNT5A Is Regulated by *PAX2* and May Be Involved in Blastemal Predominant Wilms Tumorigenesis

Yahya Tamimi*, Usukuma Ekuere*,[1], Nicholas Laughton*,[1] and Paul Grundy†

*Department of Experimental Oncology, Cross Cancer Institute, University of Alberta, 11560 University Avenue, Edmonton, Alberta, Canada T6G 1Z2; †Departments of Oncology and Pediatrics, University of Alberta, 11560 University Avenue, Edmonton, Alberta, Canada T6G 1Z2

Abstract

The *PAX2* gene encodes a transcription factor expressed during development. In humans, *PAX2* mutations cause the renal-coloboma syndrome, whereas homozygous mutations are lethal, causing severe organ malformation, notably in the brain and kidney. Wilms tumor (WT) of the kidney results from a failure in the mesenchymal-epithelial transition, a crucial step partly controlled by *PAX2*. Downstream target genes regulated by *PAX2* are still undefined. We therefore hypothesized that identification and characterization of the genes regulated by *PAX2* may improve our understanding of developmentally related malignancies including WT. We used nickel agarose chromatin enrichment, chromatin immunoprecipitation, and the human embryonic kidney–derived cell line HEK293 to identify regulatory elements responding to *PAX2*. Among others, we identified *WNT5A* as a gene potentially regulated by *PAX2*. Here, we demonstrate that *WNT5A* is a direct target of *PAX2* in HEK293 cells, using both transactivation and electrophoretic mobility shift assays. We were unable to find any *WNT5A* disease-associated mutations after screening a panel of 99 WT samples. However, quantitative reverse transcription–polymerase chain reaction in human favorable-histology WT revealed that ~66% of the cases expressed significantly less *WNT5A* than human fetal kidney. Moreover, the WiT9 WT cell line revealed a weak expression of the *WNT5A* gene. A correlation of decreased *WNT5A* expression with predominant blastemal histology tumors suggests a possible inhibitory role in WT pathogenesis. This study underlines the importance of *PAX2* in the regulation of *WNT5A*. Further *in vivo* study is necessary to determine whether the *PAX2* and *WNT5A* are truly involved in WT pathogenesis.

Neoplasia (2008) 10, 1470–1480

Introduction

Wilms tumor (WT) is the most common renal cancer affecting young children. The origin of this tumor is in the pluripotent embryonic kidney precursor cells that fail to differentiate properly during early renal development [1,2]. Pediatric kidney tumors arise in the early stem cells of the kidney and are generally responsive to chemotherapy. In contrast, cancers affecting adult kidney arise from the tubular cells and are usually highly resistant to therapy.

The association of WT with persistent foci of embryonic tissue called nephrogenic rests reflects the link with early kidney development [2]. Nephrogenic rests consist mainly of blastemal cells with varying degrees of differentiation. Interestingly, these lesions share some genetic alterations with their adjacent tumors and suspected to be precursor lesions to WT [3,4]. It is likely that genes involved in early kidney development are also involved in the initiation and progression of WT [5]. Thus, it is important to elucidate the entity and nature of the genes and mechanisms governing the differentiation of embryonic kidney stem cells.

Two transcription factors *PAX2* and *WT1* are among such genes [6–9]. *PAX2* belongs to the *paired box* gene family, characterized by a conserved domain, the *paired box* that binds specifically to DNA-binding sites to initiate regulation [10]. The functions attributed to *PAX2* in different developmental stages, including activation and/or repression of downstream genes in different cell lineages, are complex and not completely understood. In developing mammalian kidney,

Address all correspondence to: Yahya Tamimi, Cross Cancer Institute, 11560 University Avenue, Edmonton, Alberta, Canada T6G 1Z2.
E-mail: ytamimi@ualberta.ca and yahyatam@gmail.com
[1]Both authors contributed equally to this work.
Received 3 April 2008; Revised 29 September 2008; Accepted 6 October 2008

DOI 10.1593/neo.08442

PAX2 is one of the earliest markers expressed within the nephric duct and seems to orchestrate the branching of the ureteric bud through activation of glial cell line–derived neurotrophic factor (GDNF) and its corresponding receptor [11,12]. In mice, *Pax2* null mutations cause abnormal kidney development with a marked absence of ureteric bud outgrowth [13,14]. Moreover, *pax2* plays a crucial role in the mesenchyme surrounding the ureteric bud and during the early stage of epithelial differentiation [15–17]. During the apoptotic suppression process, *PAX2* seems to play an important role, particularly during the fixation of nephron number and branching morphogenesis [18–21]. Mice hemizygous for *Pax2* have reduced numbers of nephrons, less developed branching, and increased apoptosis in ureteric bud cells [19,22]. Delivery of *Bax*, a proapoptotic gene, to developing ureteric buds also reduces branching [23]. Conversely, blocking the expression of the antiapoptotic gene *bcl2* or caspases reverses the branching defects observed in mice heterozygous for the *pax2* gene [24]. At early stages of kidney development, the branching ureteric buds signal the neighboring metanephric mesenchymal cells, inducing them to aggregate and express *Pax2* while simultaneously undergoing profound changes leading to the transition from mesenchyme to epithelium. It is believed that *Pax2* expression regulates the mesenchymal-epithelial transition; however, its precise role and the downstream target genes controlled by *Pax2* are not yet known [13]. To search for evidence that *PAX2* has a direct role in WT pathogenesis, we previously used denaturing high-performance liquid chromatography (DHPLC) and sequencing analysis to screen the entire *PAX2* coding sequence for mutations. We found no evidence for disease-causing mutations, suggesting that the direct involvement of *PAX2* in WT is uncommon [25]. However, these data do not exclude the possibility that the pathway downstream from *PAX2* may be involved. Therefore, we used the nickel agarose chromatin enrichment (NACE) and chromatin immunoprecipitation (ChIP) techniques to identify genes regulated by *PAX2* [26].

In this study, we describe a possible functional role for the *PAX2* target gene, *WNT5A*. We have validated *WNT5A* as a *PAX2* target by using electrophoretic mobility shift assay (EMSA) and by polymerase chain reaction (PCR)–amplifying an enriched chromatin generated by means of ChIP technique, where an anti-Pax2 polyclonal antibody was used. We have also demonstrated that *WNT5A* is underexpressed in many favorable-histology WTs relative to fetal kidney. These data suggest a pathway where the *PAX2* gene regulates renal nephron development through WNT signaling pathway with the participation of *WNT5A* gene.

Materials and Methods

Cell Culture

Human fetal kidney cell line HEK293 was purchased from the American Type Culture Collection (Manassas, VA) and was propagated in minimum essential medium supplemented with 10% fetal bovine serum and 1% glutamine. The WT cell line WiT49, obtained recently as a kind gift from Dr. Herman Yeger (Hospital for Sick Children, Toronto, Ontario, Canada), was propagated in Dulbecco's modified Eagle's medium, containing 15% fetal bovine serum and 1% insulin. Cells were incubated at 37°C in a humidified atmosphere containing 5% CO_2, and their growth was monitored until reaching 60% to 70% confluence, at which stage the medium was changed and cells were transfected.

Transfection

HEK293 cells were transiently transfected with 4 μg of pcDNA-4/His/Max-*PAX2* DNA vector using the transfection reagent Effectine (Qiagen Inc., Valencia, CA). HEK293 cells were also transfected with an empty vector (pcDNA-4/His/Max) as a negative control. After 24 and 36 hours of incubation at 37°C in a humidified incubator containing 5% CO_2, cells were subjected to NACE or ChIP [26].

Polymerase Chain Reaction Amplification

All primers used for the PCR amplification were designed using the PRIMER3 software package (http://frodo.wi.mit.edu/cgi-bin/primer3/primer3_www.cgi) and their sequences are listed in Table 1. Amplification products were resolved on 1% agarose gel stained with ethidium bromide.

Nickel Agarose Chromatin Enrichment and ChIP

Both NACE and ChIP analyses were performed as described earlier, with slight changes in sonication time and washing stringency [26,27]. For NACE assays, HEK293 cells were fixed in their culture medium and lysed to extract and sonicate DNA five times for 20 seconds each to obtain sizes ranging between 200 and 1000 bp. Purified chromatin was then incubated with Ni^{2+} agarose beads for 6 hours and washed, and DNA/protein complexes were purified as described earlier [26]. After reversing the cross-linking of the complexes formed by DNA/proteins, DNA was purified through Qiagen columns after a complete digestion of proteins. We recently succeeded to optimize conditions for a specific anti-Pax2 antibody used in ChIP that was carried out exactly as described above for NACE with the exception of replacing Ni^{2+} with a polyclonal Pax2 antibody and a final purification through phenol chloroform extraction [26,28]. A mouse IgG polyclonal antibody was used as a negative control for ChIP assays.

Cloning and Sequencing of the NACE-Enriched Chromatin

Five hundred nanograms of the enriched DNA was end-filled and ligated to the *Eco*RV-digested pBluescript II SK(–) vector (Stratagene, La Jolla, CA). Ligation products were used to transform XL-Blue competent cells, and DNA from putative-positive clones was extracted. Enzymatic digestions confirmed the presence of the insert, and positive clones were sequenced on an automated sequencer (CEQ8000 Genetic Analysis System; Beckman Coulter, Mississauga, Ontario, Canada) using dye terminator cycle sequencing chemistry (Beckman Coulter).

Construct Preparation

The *PAX2* cDNA encoding the entire open reading frame was subcloned into *Eco*RI-*Xba*I sites in the pcDNA4-His/Max plasmid

Table 1. Sequence of Primers Used for PCR Assays.

Forward	Reverse
5′-GAG GAG AAG CGC AGT CAA TC-3′	5′-GAA GAG GAA GAA CAC GCA CA-3′
5′-CCA CCT CGA GAT TTC ACG TA-3′	5′-TTT TCC TAC CTA TCT GCA TCA CC-3′
5′-GCC AGT GAT CCC TTG TCC T-3′	5′-GGG CAA GGT GAG AAG ACA GA-3′
5′-CAT CTG GCT CCT CCA TGA AT-3′	5′-GGT GGC ACC CAC TAC TTG-3′
5′-ATG AGT CCA ACA TGC AGA GA-3′	5′-GTA ACT GTA TCA GTG AAA AT-3′
5′-ATG AGT CCA ACA TGC AGA GA-3′	5′-GTT GGC AGG CAC AGC TGG TT-3′
5′-AAC CAG CTG TGC CTG CCA AC-3′	5′-GTA ACT GTA TCA GTG AAA AT-3′

The PCR conditions were optimized to amplify a specific band of expected size using DNA samples as templates. The NACE-enriched *WNT5A* 5′-upstream element (AB) was amplified totally or partially (subfragments A and B) before cloning.

Table 2. Sequence of Oligonucleotides Used for EMSA.

Oligos	Sense—Biotin-Labeled	Antisense
P2BS	5′-TTC GTG GTC ATG TAA GTT GTT TCA CTT GGA TGA AAT CCC TCT TCA GGA GAT GTT-3′	5′-AAC ATC TCC TGA AGA GGG ATT TCA TCC AAGTGA AAC AAC TTA CAT GAC CAC GAA-3′
α	5′-ATG AGT CCA ACA TGC AGA GAG AAG CAG AGA-3′	5′-TCT CTG CTT CTC TCT GCA TGT TGG ACT CAT-3′
β	5′-GAA GCA GAG AAG AGA GAT GAA TGC AAC AGG-3′	5′-CCT GTT GCA TTC ATC TCT CTT CTC TGC TTC-3′
γ	5′-ATG CAA CAG GGG TGG GAG AGA TGG AAA GAT-3′	5′-ATC TTT CCA TCT CTC CCA CCC CTG TTG CAT-3′
δ	5′-ATG GAA AGA TAG AGA GAT AGA CAG AGA CAG-3′	5′-CTG TCT CTG TCT ATC TCT CTA TCT TTC CAT-3′
ε	5′-ACA GAG ACA GAG GCA GAG AGA TCT GAG AAC-3′	5′-GTT CTC AGA TCT CTC TGC CTC TGT CTC TGT-3′
ζ	5′-ATC TGA GAA CCA GCT GTG CCT GCC AAC-3′	5′-GTT GGC AGG CAC AGC TGG TTC TCA GAT-3′
γ′	5′-TAC GTT GTC CCC ACC CTC TCT ACC TTT CTA-3′	ATG CAA CAG GGG TGG GAG AGA TGG AAA GAT-3′

(Invitrogen, Carlsbad, CA). The *WNT5A* 5′-upstream enriched fragment (AB) of ~300 bp was amplified and cloned first into pGEM-T-easy vector (Promega, Madison, WI) and subsequently subcloned upstream of the luciferase gene in the pGL3 vector (Promega). The AB fragment was subdivided by PCR amplification into units, A and B, of ~155 and ~145 bp, respectively. The fragments were subcloned upstream to the luciferase reporter in pGL3 vector as described above. A synthesized fragment (P2BS1) of 54 bp, containing a confirmed *PAX2* binding site [29], was end-filled, cloned upstream to the cytomegalovirus promoter of the pGL3 vector, and used as a positive control for transactivation.

Transactivation Assays

We amplified fragment AB covering the total ~300 bp as well as overlapping fragments A and B, which, together, covered the total region of ~300 bp. The three amplicons A, B, and AB were each cloned into a TA vector-sequenced and subcloned into pGL3-CMV-luciferase reporter vector. HEK293 cells were cultured in 12-well plates at a density of 1×10^5 cells/ml and cotransfected 36 hours later with *PAX2*-pcDNA4-His/Max or pcDNA4-His/Max and 300 ng of pGL3 vector containing either the *PAX2* binding site or fragments A, B, and AB placed upstream of the Luciferase gene in pGL3. Twenty-four hours later, cells were harvested and subjected to luciferase activity–monitoring according to the manufacturer's guidelines (Promega). A reporter construct containing one *PAX2* binding site [29] (P2BS-pGL3, see sequence in Table 2) was used as positive control. For each set of experiments, transfections were performed in triplicates and repeated three times for confirmation.

Electrophoretic Mobility Shift Assays

In addition to the P2BS oligonucleotides containing the *PAX2* binding site, six overlapping oligonucleotides (α, β, γ, δ, ε, and ζ) covering the total sequence of the A fragment were synthesized (Table 2) with one strand conjugated to biotin. HEK293 cells expressing endogenous and recombinant *PAX2* proteins were lysed, and protein extracts were resolved on 6% polyacrylamide Tris-glycine-EDTA. Five micrograms of protein extracts was incubated with 1.3 mM DTT, 5 μg of sheared salmon sperm DNA, 1 μg of poly dIdC (Sigma, St. Louis, MO), and biotin-labeled oligonucleotides (α, β, γ, δ, ε, and ζ) as well as P2BS fragments. Samples were incubated at room temperature for 20 minutes to form protein-DNA complexes. After 45 minutes of a prerun of the gel, samples were analyzed by electrophoresis. Protein-DNA complexes were subsequently transferred to a membrane, and signals were revealed by using a chemiluminescent nucleic acid detection module (Pierce, Rockford, IL).

Supershift Assay

Ten micrograms of HEK293 protein extract was incubated overnight with 2 μg of anti-Pax2 antibody (Santa Cruz Biotechnology, Santa Cruz, CA) in 12 μl of 5% skim milk. Biotin-labeled probes were subsequently added and incubated for another 20 minutes at room temperature. Samples were resolved on a 5% acrylamide gel using 1× TGE buffer (50 mM Tris, 380 mM glycine, and 2 mM EDTA, pH 8.2) at 4°C for 1.5 hour using 20 mA. The transfer and the detection of the signal were performed as above for EMSA.

Silencing of PAX2 *and* WNT5A

Two oligonucleotides designed for each of the two genes *PAX2* and *WNT5A* to specifically knock down their expression, were purchased from Qiagen and their sequences are as follow: *PAX2*-siRNA$_1$ 5′-CACAGCTACACGCCCATTAAA-3′; *PAX2*-siRNA$_2$ 5′-CCCGTAGTTGCTCTTTCGGTA-3′; *WNT5A*-siRNA$_2$ 5′-CCGGATAACCTTGTAACATAT-3′; *WNT5A*-siRNA$_6$ 5′-TTGG-TGGTCGCTAGGTATGAA-3′. siRNA duplexes were transfected into WiT49 cells using HiPerFect (Qiagen) according to the manufacturer's instructions. Cells were plated into 60 mm and/or six-well dishes at a density of 5×10^4 cells/ml 24 hours before transfections. A total of 5 μl of 20 μM siRNA solution and 20 μl of the transfection reagent HiPerFect (Qiagen) were incubated with 0.5 ml of serum-free Dulbecco's modified Eagle's medium for 10 minutes before adding the resulting mixture to the cells dropwise. For data confirmation, each siRNA transfection was processed in duplicate.

Protein Extraction and Western Blot

Twenty-four hours of incubation after transfection, cells were rinsed twice with cold phosphate-buffered saline and lysed in protein lysis buffer (20 mM *N*-2-hydroxyethylpiperazine-*N*′-2-ethanesulfonic acid pH 7.6, 75 mM NaCl, 2.5 mM $MgCl_2$, 0.1 mM ethylenediaminetetraacetic acid, 0.1% Triton X-100, 1 μg/ml leupeptin, 1 μg/ml aprotinin, 1 μg/ml pepstatin, and 1 mM phenylmethylsulfonyl fluoride). The cell lysates were kept on ice for 10 minutes, rotated at 4°C for 20 minutes, and centrifuged at 10,000 rpm for 15 minutes, and the supernatant was subjected to Bradford protein assay using a BioRad kit (Bio-Rad, Hercules, CA) to determine protein concentrations using bovine serum albumin as a standard control. Equal amounts of proteins from each set of experiments were loaded on a 6% acryl/bisacrylamide gel. Because *WNT5A* is a secreted protein, its detection required the collection of the medium at 24 hours of incubation after transfection, then concentration through a "centricon" concentrator column and quantification.

The protein extracted from WiT49 cells or concentrated medium were resolved on 10% polyacrylamide gel and transferred to a nitrocellulose membrane. Immunoblot analyses for Pax2 and Wnt5a proteins were performed with rabbit polyclonal and monoclonal antibodies respectively (cell signaling, dilution of 1:150). Immunoblots were incubated overnight at 4°C and followed by 2 hours of incubation at room temperature with an HRP-conjugated antirabbit IgG secondary antibody (dilution 1:5000; Cell Signaling, Danvers, MA). Generated signals were revealed by chemiluminescent protein detection kit (Pierce).

In Silico *Analysis*

Both Ensembl (http://www.ensembl.org/index.html) and National Center for Biotechnology Information (NCBI; http://www.ncbi.nlm.nih.gov/) Web sites were used for the BLAST analysis of the relevant clones, for the screening of the nucleotide databases for other species, and for the localization of regions similar to the *WNT5A* upstream element [30]. Similar sequences from human and mouse were aligned using the NCBI Web site.

Mutation Analysis

DNA preparation and mutational analysis were performed as described earlier [25]. DNA samples from 99 favorable-histology WT cases were obtained from the Renal Tumors Bank of the Children's Oncology Group [31] after approval from our institutional research ethics committee. Exons 1 to 4 of the human *WNT5A* were subjected to PCR amplification using the panel of primers listed in Table 1. For each WT sample, a wild type DNA control was amplified in parallel under the same conditions. The specificity of the PCR products was monitored by electrophoresis on a 1.5% agarose gel.

For DHPLC analysis, 10 μl of PCR product from each WT and from the wild type were mixed together, heated to 95°C for 5 minutes, and cooled to 25°C at a rate of 1.5°C/min. Denaturing high-performance liquid chromatography analysis was performed using the WAVE nucleic acid fragment system (Transgenomics, Omaha, NE) equipped with a L7300+ column oven using a DNA Sep column as described earlier [25].

Quantitative Reverse Transcription–Polymerase Chain Reaction and Statistical Analysis

Thirty-eight frozen tissue samples of favorable-histology WT were subjected to total RNA extraction using TRIzol reagent (Life Technologies, Gaithersburg, MD). After DNase treatment, 5 μg of each RNA sample was run on a denaturing agarose gel, and the quality of RNA was monitored under UV light using ethidium bromide staining of the gel. cDNA was produced using 0.5 μg of RNA with the SuperScript II Reverse Transcriptase (Invitrogen). Quantitative PCRs were carried out using the 7900HT Fast Real-Time PCR systems (Applied Biosystems, Foster City, CA) and performed following the guidelines provided by the company (Applied Biosystems) using the *Taq*Man Gene Expression Assay Kit. All cDNA samples were assayed in triplicate for each primer set. Primers to amplify ~140-bp fragments of *WNT5A* and *GAPDH* genes together with specific probe for each gene were included in the 20× *Taq*Man Gene Expression Assay Mix (Applied Biosystems). Expression data normalized to *GAPDH* and fetal kidney controls were analyzed using the $\Delta\Delta C_t$ method [32]. The Children's Oncology Group Renal Tumors Reference Pathologist categorized tumor histology.

Results

Nickel Agarose Chromatin Enrichment Generates Potential Candidate Genes Regulated by PAX2

At the start of this project, we were unable to find a highly specific Pax2 antibody as required in ChIP analysis. Thus, we used the NACE technique, an antibody-free affinity-enrichment method based on Ni^{2+}-NTA affinity chromatography, a variant of ChIP that can be used as an alternative to overcome the lack of a specific antibody and nonspecific cross-linking [26]. We have used the human embryonic kidney cell line HEK293 as a model system to identify gene targets of *PAX2* and its regulation of gene expression. Pax2 protein expression was detectable by Western blot in HEK293 cells (Figure 1*A*), making it an appropriate model to isolate and test the predicted *PAX2*-target regulatory elements.

DNA fragments from 140 *PAX2* NACE clones were sequenced and BLAST-searched in public sites at NCBI (http://www.ncbi.nlm.nih.gov/) and Ensembl (http://www.ensembl.org/index.html). BLAST analysis revealed DNA sequences related to 1 adhesion molecule, 23 novel genes, 5 proto-oncogenes, and 11 transcription factors including *WNT5A*, *WT1*, *WIT1*, and the *SOX11* genes. The remaining 76 clones were repetitive sequences or could not be sequenced and were excluded from further investigations. Table 3 lists the NACE-generated putative regulatory elements binding to *PAX2*. Whereas the identification of genes such as *WT1*, previously described as a *PAX2*-target gene supports the specificity of the NACE procedure, validation experiments were, nevertheless, undertaken for candidate

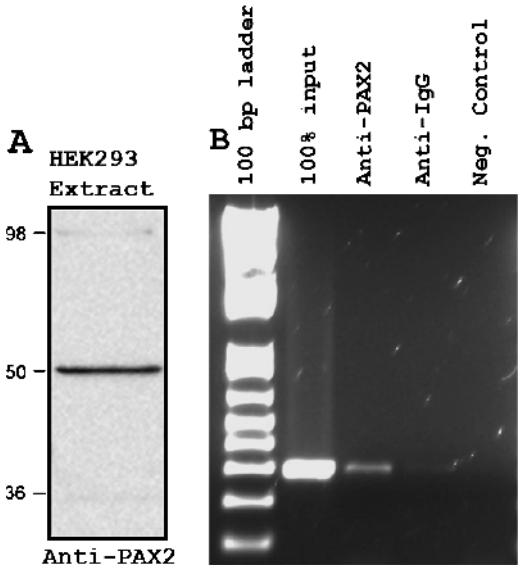

Figure 1. Endogenous *PAX2* binds to *WNT5A* 5′-upstream region. (A) Western analysis of Pax2 protein expression in HEK293 cells nuclear extract. (B) Chromatin immunoprecipitation was performed using a polyclonal antibody directed against Pax2. The enriched chromatin was amplified using primers flanking the NACE enriched *WNT5A* 5′-upstream region. A specific band of an expected size (~300 bp) was obtained in the sample treated with the anti-Pax2 antibody but not in samples treated with an anti-IgG or mock controls.

Table 3. Recapitulation of NACE-Generated Regulatory Elements Presumably Interacting with *PAX2*.

No. and Gene Symbol	Locus	Category	No. and Gene Symbol	Locus	Category
01. *ABLIM3*	5q33.1	Adaptor	33. *BIRC6*	2p22.21	Protooncogene
02. *CIB1*	15q25.3-q26	Adhesion	34. *HRB2*	12q21.1	Protooncogene
03. *CD4*	12p13.31	Antigen	35. *EIF2C4*	1p34.3	Protooncogene
04. *VRK2*	2p16-p15	Enzyme	36. *NOT4*	7q33	Transcription factors
05. *MAP2K5*	15q22.2-31	Enzyme	37. *RNF39*	6P21.3	Transcription factors
06. *GUCY1B2*	13q14.2-14.3	Enzyme	38. *SOX11*	2P25.3	Transcription factors
07. *DPP10*	2q14.1	Enzyme	39. *ZNF141*	4p16.3	Transcription factors
08. ?	Chromosome #9	Novel/hypothetical	40. *BTG4*	11q23.2-3	Transcription factors
09. ?	1q41	Novel/hypothetical	41. *N6AM1*	21q22.1	Transcription factors
10. ?	XP11.22	Novel/hypothetical	42. *GTF2B1*	1p22.1-3	Transcription factors
11. ?	Chromosome #17	Novel/hypothetical	43. *ARHGAP8*	22q13.31	Transcription factors
12. ?	9p24.1	Novel/hypothetical	44. *WT1* and *WIT1*	11p13	Transcription factors
13. ?	Chromosome #20	Novel/hypothetical	45. *TCF4*	18q21.1	Transcription factors
14. ?	Chromosome #12	Novel/hypothetical	46. *MAFK*	7p22	Transcription factors
15. ?	Chromosome #22	Novel/hypothetical	47. *ELL2*	5q15	RNA Associated
16. ?	1p32.1	Novel/hypothetical	48. *NXT1*	20p12	RNA Associated
17. ?	Chromosome #7	Novel/hypothetical	49. *SRRM2*	16P13.3	RNA Associated
18. ?	Chromosome #1	Novel/hypothetical	50. *HTR1E*	6q14-15	Signaling/receptor
19. ?	Chromosome #4	Novel/hypothetical	51. *MAPKAP1*	9q34.11-12	Signaling/receptor
20. ?	18q21.1	Novel/hypothetical	52. *DCAMKL1*	9q34.11-12	Signaling/receptor
21. ?	Chromosome #2	Novel/hypothetical	53. *DLG2*	11q	Signaling/receptor
22. ?	11q14.1	Novel/hypothetical	54. *CCKAR*	4p15.2	Signaling/receptor
23. ?	22q122.1	Novel/hypothetical	55. *AKAP13*	15q24-25	Signaling/receptor
24. ?	21q21	Novel/hypothetical	56. *TNFSF4*	1q24-25	Signaling/receptor
25. ?	15q23	Novel/hypothetical	57. *GEF6*	Chromosome X	Signaling/receptor
26. ?	3q26.31	Novel/hypothetical	58. *PTPRM*	18P11.2	Signaling/receptor
27. ?	Chromosome #4	Novel/hypothetical	59. *HARP*	Chromosome #16	Signaling/receptor
28. ?	Chromosome #7	Novel/hypothetical	60. *TNFRSF9*	1p36	Signaling/receptor
29. ?	Chromosome #9	Novel/hypothetical	61. *ACTRT1*	X26.1	Structural protein
30. ?	16q21-22.1	Novel/hypothetical	62. *SH120*	1P36.13	Structural protein
31. *WNT5A*	3p21.1	Protooncogene	63. *ABLIM3*	5q33.1	Structural protein
32. *SEMA3E*	7q21.11	Protooncogene	64. *FAM36A*	1q44	?

genes, which we intended to characterize (Figure 2). Owing to the known central role of the *WNT* pathway in the development of the kidney, we chose to further analyze the *WNT5A* gene first.

Confirmation of WNT5A *As a Target Regulated by* PAX2

To determine whether endogenous *PAX2* binds to the *WNT5A* promoter *in vivo*, we performed ChIP analysis using HEK293 cells, and an antibody, which conditions for specific binding to endogenous *PAX2*, were recently optimized. Western blot analysis, using HEK293 cells, protein extracts showed a specific band of an expected size of ~50 kDa, consistent with the molecular weight of *PAX2* (Figure 1*A*). As shown in Figure 1*B*, a ~300-bp fragment located upstream of *WNT5A* containing the putative *PAX2* binding site was amplified from *PAX2* immunoprecipitates, indicating that endogenous *PAX2* binds to the putative *WNT5A* regulatory region. Additionally, amplification of the ~300-bp fragment using the ChIP product as template confirms the specificity of the NACE-enriched fragment, corresponding to a regulatory element mapped ~82 kb upstream of the *WNT5A* gene.

Transactivation Assays

To prove whether the NACE- and ChIP-derived ~300-bp *WNT5A* upstream fragment possessed a *PAX2*-responsive element, a transactivation assay was performed. Monitoring luciferase activity revealed that *PAX2* significantly enhanced the expression from all *WNT5A* upstream element luciferase reporters, A, B, and AB (Figure 3). *PAX2*-enhanced luciferase expression was greatest when cotransfected with fragment A, whereas AB fragment expression was similar to the P2BS control. The pGl3 empty vector was used as a negative control.

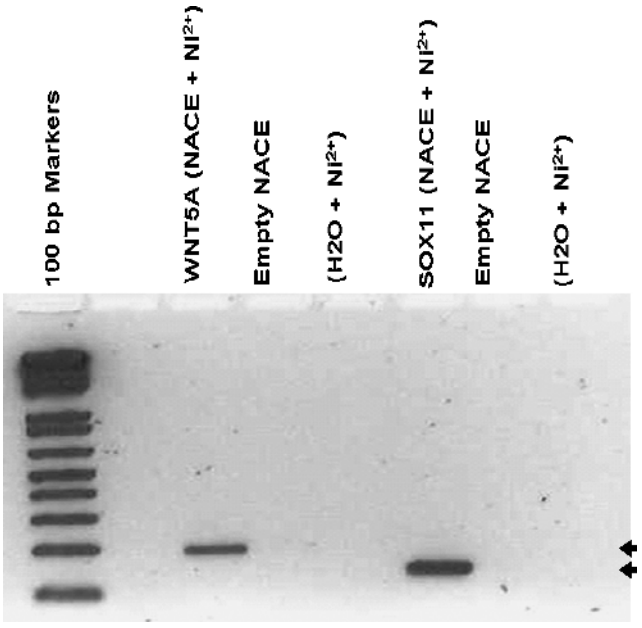

Figure 2. Validation of NACE specificity. A representative example of PCR amplification using NACE product as template and primers designed to amplify the 5′upstream region of *WNT5A* and *SOX11* genes. Both *WNT5A* and *SOX11* were confirmed to be specifically present in the *PAX2* NACE product. Bands of the expected sizes were obtained (arrows) specifically in *PAX2*-transfected samples enriched by NACE. Material enriched from HEK293 cells transfectd by an empty vector was used as a control along with water and Ni^{2+} agarose beads (mocks).

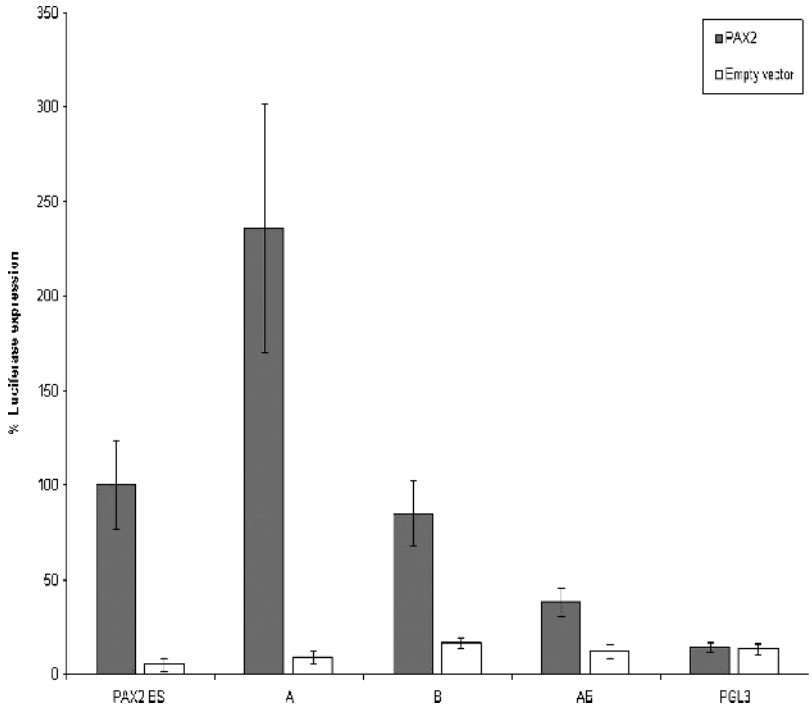

Figure 3. Transactivation assays of the *WNT5A* 5′-upstream region. The ~300-bp NACE-enriched fragment (AB) and subfragments A and B were cloned into the pGL-3 CMV luciferase vector. The three vectors were cotransfected with pcDNA-4/His/Max-*PAX2* expression vector and pRL-CMV internal control plasmid into HEK293 cells. Dual-luciferase activity ratios were calculated relative to express-tagged *PAX2* activation of P2BS, the *PAX2* binding site reporter. Error bars, SEM.

Electrophoretic Mobility Shift Assays

Based on data obtained with the transactivation assays, fragment A was suspected to contain the binding site of *PAX2*. Six overlapping biotin-labeled oligonucleotides (α, β, γ, δ, ε, and ζ), covering fragment A as well as the *PAX2* binding site P2BS, were synthesized (Table 2). A protein extract from HEK293 cells was incubated with each oligo, and reactions were resolved on a 10% polyacrylamide gel. In addition to that observed with the P2BS oligo, a clear shift was obtained only with the gamma-oligo (γ) (Figure 4*A*) indicating that the binding site is likely located within this 30-bp sequence. The synthesis of an oligo gamma′ (γ′) where pyrimidines were replaced by purines and purines by pyrimidines eliminated the observed shift (Figure 4*A*).

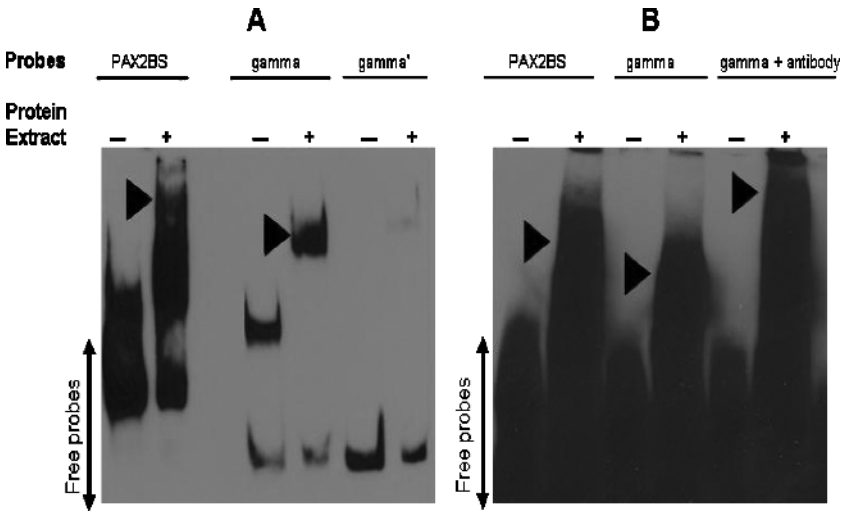

Figure 4. *PAX2* binding to sequences in the *WNT5A* 5′-upstream region. Electrophoretic mobility shift assay to assess the direct binding of *PAX2* to potential sequences including a synthetic control binding site (P2BS), the *PAX2* binding site from the *PAX2* 5′-upstream region (gamma-γ), and the same sequence altered by changing purines to pyrimidines and vice versa (gamma′-γ′). (▶) Arrowheads indicate shifts caused by proteins-probes complex formation (A). An anti-Pax2 antibody was added to the complex formed between protein extracts and biotin-labeled gamma oligos to validate the specificity of the binding. A supershift migrating at higher molecular weight was observed (B).

To validate the specificity of the binding, we optimized conditions for a supershift assay using a specific antibody to Pax2 protein. A detectable label migrating at higher apparent molecular weight was observed as a result of the anti-Pax2 antibody binding with the biotin-labeled probes/protein extracts' heterocomplexes (Figure 4*B*).

In Vitro *siRNA-Mediated Silencing of* PAX2 *and* WNT5A

To knock down *PAX2* and *WNT5A* genes, we used siRNA formulations commercialized by Qiagen and optimized to efficiently shut down the expression of *PAX2* and *WNT5A*. WiT49 cells were transfected by either *PAX2*-siRNA$_1$/*PAX2*-siRNA$_2$ or *WNT5A*-siRNA$_2$/*WN5A*-siRNA$_6$ sets. Cotransfection with both sets (*PAX2*-siRNA$_1$ and *PAX2*-siRNA$_2$ or *WNT5A*-siRNA$_2$ and *WN5A*-siRNA$_6$) was highly toxic to the cells. An siRNA with no specific binding to human, mouse, and rat (sequence not revealed by the company) was used as a negative control (Figure 5*A*). siRNA-treated samples were subjected to Western analysis using antibodies directed against Pax2, Wnt5a, and β-actin as loading controls. All the four siRNA significantly contributed to a successful knock down of *PAX2* and *WNT5A* expression (Figure 5, *B* and *C*). For *PAX2* knock down, siRNA$_2$ looks slightly more efficient than siRNA$_1$ (Figure 5*B*), whereas for *WNT5A* gene, siRNA$_2$ seems more effectual than siRNA$_6$ (Figure 5*C*). β-Actin monitoring of the treated samples showed that the observed knock down was not caused by an eventual loss of the material but by siRNA treatment (Figure 5, *B* and *C*).

Mutation Screenings of WNT5A *in WT Patients*

The four exons covering the entire coding sequence of *WNT5A* were amplified separately using primers listed in Table 1 and were subjected to mutation analysis using DHPLC. None of the 99 WT samples displayed a chromatogram with abnormal pattern when compared to their control DNA samples, providing no evidence for exon-specific mutations in *WNT5A* in WTs.

Quantitative Reverse Transcription–Polymerase Chain Reaction

To assess the expression profile of *WNT5A* in WT samples, we performed quantitative reverse transcription–polymerase chain reaction

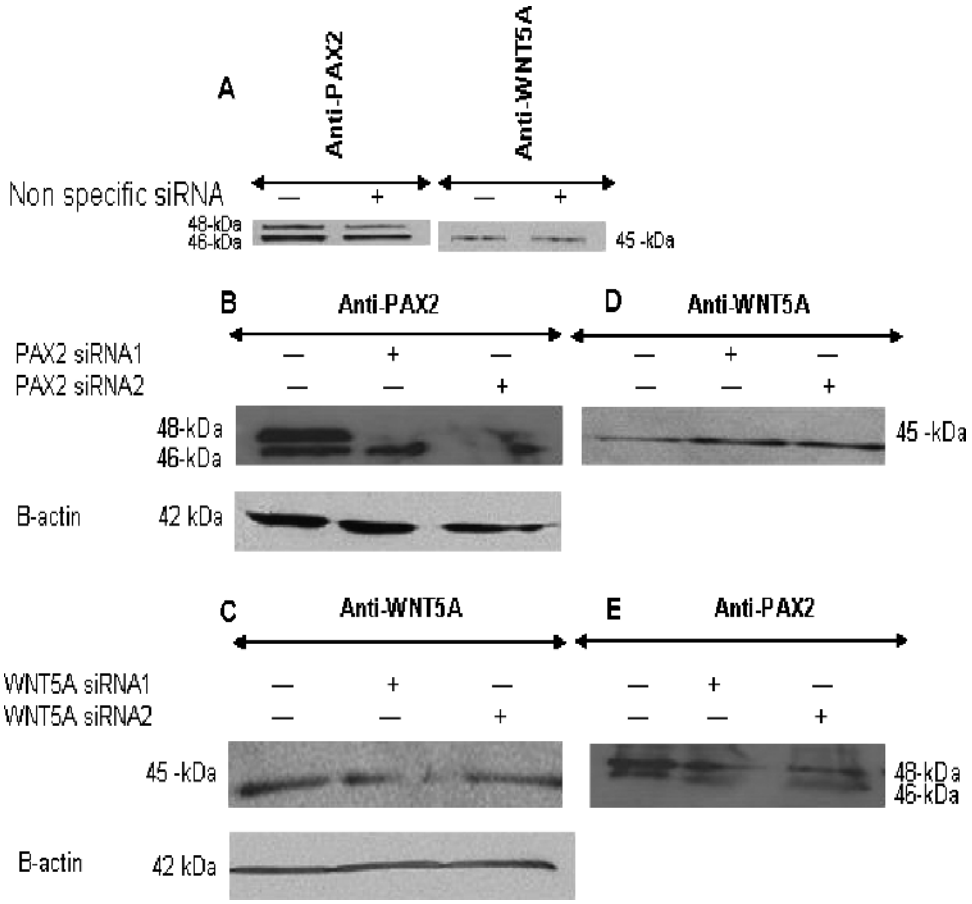

Figure 5. siRNA-based knock down of *PAX2* and *WNT5A* genes. Two locations within *PAX2* and *WNT5A* genes were specifically targeted to knock down their expression using commercialized siRNA (Qiagen). A nonspecific siRNA was used as a negative control where protein expression is not altered in treated samples compared to nontreated samples (A). It is noteworthy that *WNT5A* expression is weak when compared to the *PAX2* expression in the WiT49 WT cell line. Both *PAX2*-siRNA$_1$ and *PAX2*-siRNA$_2$ were efficient to reduce drastically *PAX2* expression (B), whereas *WNT5A* expression was clearly detectable in the same samples (D). Culture medium where WiT49 cells were propagated and treated with *WNT5A*-siRNA$_2$ and *WNT5A*-siRNA$_6$ was concentrated and subjected to Western blot analysis using an anti-Wnt5A antibody. Like *PAX2*-siRNA, both *WNT5A*-siRNA$_2$ and *WNT5A*-siRNA$_6$ reduced the *WNT5A* expression (C). The presence of *PAX2* expression was detected in these *WNT5A* knocked down samples (E).

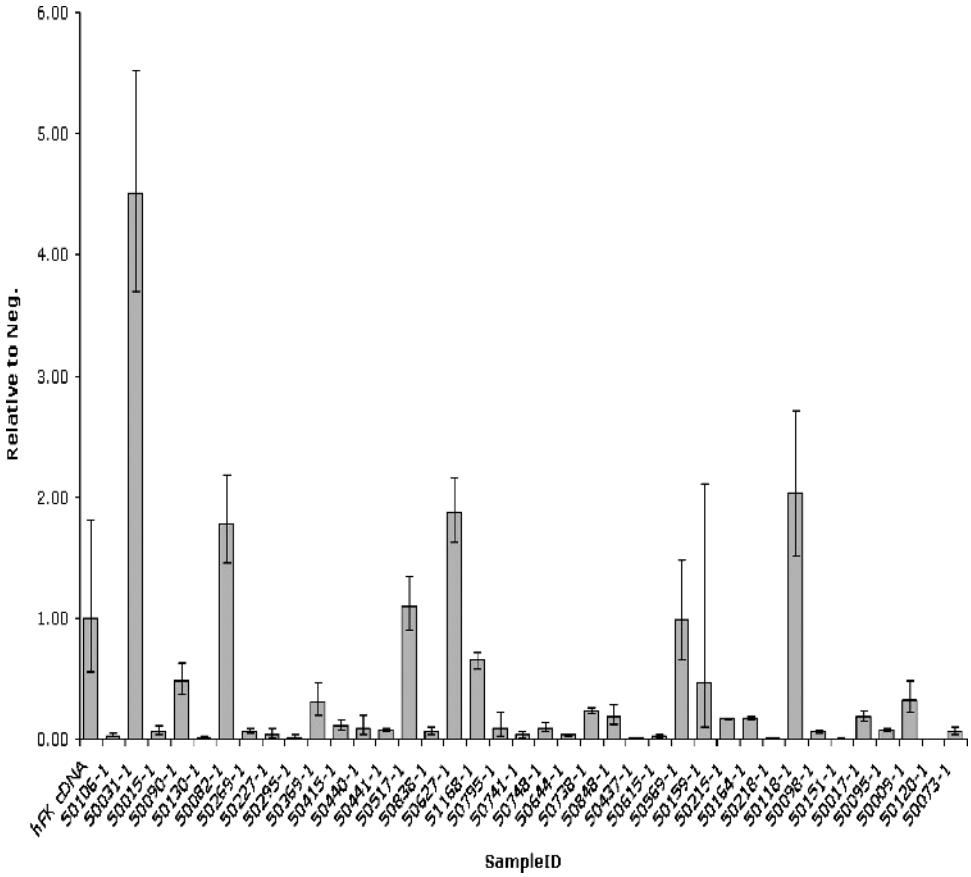

Figure 6. Quantitative RT-PCR to assess the expression levels of *WNT5A* in WT samples of favorable-histology. Gene expression assay (Applied Biosystems) was performed on 38 WT samples. Human fetal kidney was included as a control to which all data were normalized. Error bars, relative SE.

(RT-PCR) using the *Taq*Man Gene Expression Assay from Applied Biosystems on RNA isolated form favorable-histology WT samples. Of the 38 cases tested, 25 showed significantly less expression of *WNT5A* compared to the human fetal kidney control (Figure 6 and Table 4). Exceptionally, one sample highly overexpressed *WNT5A* relative to fetal kidney, whereas the expression levels in the remaining 12 cases were not significantly different from fetal kidney.

We subsequently examined the relationship between *WNT5A* expression and tumor histology. Samples were categorized in *WNT5A* expression as either aberrant or normal and compared to histologic classification based on predominant histologic finding; that is, blastemal, epithelial, or stromal as determined on central pathology review on Children's Oncology Group study AREN03B2 (Table 4). Fifteen samples showed predominant blastemal histology, two samples showed predominant epithelial histology, and the remainder showed predominantly stromal histology. Using the McNemar exact test for nonparametric data, a significant correlation between *WNT5A* underexpression and predominant blastemal histology was observed (P = .000122, n = 14/38).

Discussion

We used the HEK293 cell line to identify target genes regulated by *PAX2*, a transcription factor known for its role in kidney development [33]. Our preliminary experiments revealed that this cell line expresses *PAX2*, making it an appropriate model to isolate and test the predicted target regulatory elements. In contrast to most cancers where both animal models and cell lines are available, the study of WT still suffers from the lack of good cell line models. The few WT lines that have been reported, including WiT49 and HWFT, usually harbor a *p53* mutation, characteristic of the anaplastic variant of WT and likely not representative of the much more common favorable-histology WT (95% of WTs are favorable histology), which rarely includes mutation of the *p53* gene [34,35]. We chose HEK293 cells as a very well characterized line, which is easily used for transfection/transactivation assays, especially for its human embryonic kidney origin. However, findings generated by using this model remain speculative because a good cell line representing favorable-histology WTs have not yet been established.

BLAST sequence analysis of the *PAX2* NACE-derived sequences revealed responsive elements from a variety of genes including adhesion proteins, proto-oncogenes, transcription factors, and some novel genes (Table 3). Approximately 54% of the clones (76/140) were either repetitive sequences or could not be sequenced and were excluded from further analysis.

Among the potential *PAX2* targets obtained using the NACE and ChIP techniques, a ~300-bp *WNT5A* 5′-upstream element was particularly interesting. WNT genes are expressed in a variety of human tissues, including bladder and fetal kidney, and, therefore, play a major role in kidney development [33] and is implicated in cancer [36]. The NACE-enriched fragment, localized ~82 kb upstream of the *WNT5A* gene, is conserved between human and mice and repre-

Table 4. Expression Analysis and Histology Classification for the 38-Sample Experimental Set.

Sample	ID No.	ΔC_t	σ	Test Statistic	*P*	Significance [$\alpha < 0.05$]	Histology Classification
Control	HFK cDNA	10.27	0.86	0	1	No	–
1	50106-1	15.30	0.69	7.919	.02	Yes	Epithelial
2	50031-1	8.09	0.29	4.155	.05	Yes*	Epithelial
3	50015-1	14.23	0.74	6.047	.03	Yes	Blastemal
4	50090-1	11.33	0.38	1.954	.19	No	Stromal
5	50130-1	16.94	1.24	7.657	.02	Yes	Blastemal
6	50082-1	9.44	0.29	1.582	.25	No	Stromal
7	50269-1	14.30	0.40	7.369	.02	Yes	Stromal
8	50227-1	14.93	1.17	5.565	.03	Yes	Blastemal
9	50295-1	17.01	2.12	5.106	.04	Yes	Stromal
10	50369-1	11.98	0.61	2.825	.11	No	Stromal
11	50415-1	13.42	0.50	5.505	.03	Yes	Stromal
12	50440-1	13.81	1.21	4.147	.05	Yes	Stromal
13	50441-1	13.99	0.28	7.143	.02	Yes	Stromal
14	50517-1	10.13	0.29	0.266	.82	No	Stromal
15	50838-1	14.27	0.71	6.223	.02	Yes	Blastemal
16	50627-1	9.36	0.20	1.776	.22	No	Stromal
17	51168-1	10.89	0.15	1.25	.34	No	Stromal
18	50795-1	13.89	1.44	3.742	.06	No	Blastemal
19	50741-1	15.24	0.92	6.842	.02	Yes	Blastemal
20	50748-1	13.73	0.63	5.648	.03	Yes	Blastemal
21	50644-1	15.20	0.33	9.291	.01	Yes	Blastemal
22	50738-1	12.38	0.14	4.21	.05	Yes	Blastemal
23	50848-1	12.69	0.58	4.035	.06	No	Blastemal
24	50437-1	17.07	0.13	13.57	.01	Yes	Blastemal
25	50615-1	15.92	0.71	8.768	.01	Yes	Blastemal
26	50569-1	10.30	0.59	0.048	.97	No	Stromal
27	50159-1	11.36	2.17	0.813	.5	No	Stromal
28	50215-1	12.85	0.10	5.183	.04	Yes	Stromal
29	50164-1	12.78	0.11	5.039	.04	Yes	Stromal
30	50218-1	17.60	0.04	14.789	0	Yes	Blastemal
31	50118-1	9.24	0.42	1.854	.2	No	Stromal
32	50098-1	14.34	0.26	7.871	.02	Yes	Stromal
33	50151-1	17.99	0.44	13.88	.01	Yes	Stromal
34	50017-1	12.71	0.37	4.533	.05	Yes	Stromal
35	50095-1	14.04	0.16	7.494	.02	Yes	Blastemal
36	50009-1	11.88	0.56	2.733	.11	No	Stromal
37	50120-1	17.83	0.09	15.176	0	Yes	Stromal
38	50073-1	14.28	0.62	6.547	.02	Yes	Stromal

*This sample showed significant over expression (Figure 1).

sents one of the upstream noncoding putative regulatory regions (Figure 7). Likewise, the identified ~300 bp lies within an area belonging to other genes located in the vicinity, notably within the last intron of *ERC2* gene, upstream the *WNT5A*. Owing to its central position in several developmental pathways and its involvement in the control of different steps in certain organs' formation including the kidney [13], *PAX2* can adopt polyvalent functions and has the capacity to interact simultaneously with different entities.

The results of our transactivation experiments demonstrated that the *WNT5A* upstream element was sufficient to provide *PAX2*-dependent activation of gene expression and led to the identification of an authentic *PAX2* responsive element within the 155-bp subfragment of the *WNT5A* 5′-upstream element (Figure 3). The fragment contains a DNA sequence to which *PAX2* binds specifically as shown by EMSA and confirmed by the supershift assay (Figure 4*B*). Moreover, mutations of (γ), the fragment harboring the putative *PAX2* binding site, resulted in a complete removal of the observed shift (Figure 4*A*). Surprisingly, the subfragment A displayed the highest luciferase expression activity compared to the positive control (PAX2BS) and particularly to the total fragment AB of ~300 bp (Figure 3). This discrepancy might be caused by the presence of an inhibitory element in fragment AB, which is not present in the smaller fragment A (Figure 3).

Because we found that *WNT5A* is a direct target of the *PAX2* gene, which itself interacts reciprocally with *WT1*, and because *WT1* is known to be involved in approximately 15% of sporadic WTs [37], we tested whether mutations of *WNT5A* could be detected in WTs. The analysis of a panel of 99 WT samples revealed no disease-associated mutations, however, indicating that mutation of *WNT5A* itself is unlikely to be a significant cause of WT.

Interestingly, however, the expression levels of *WNT5A* in favorable-histology WTs, assessed by quantitative RT-PCR, showed that approximately two-thirds of the cases displayed significantly less *WNT5A* expression than human fetal kidney control (Figure 6). Furthermore, there seemed to be a significant correlation between low *WNT5A* expression levels and categorization of the tumors as having predominantly blastemal histology.

The development of the metanephric kidney is at least a two-step process in which the undifferentiated metanephric mesenchyme is rescued from apoptosis by the developing ureteric bud and subsequently triggered into a mesenchymal-epithelial conversion to form the mature nephron [38]. Tissue that has been rescued from the apoptotic fate, but is to receive the second transition signal, is often termed the *metanephric blastema*. In general, the first transition occurs in cells proximal to the invading ureteric bud, whereas subsequent transitions are observed after primary and secondary branchings have occurred. Thus, the topography of the developing kidney is reflective of its chronological maturity, with the "earliest" developmental stages occurring near the outer edges around the buds of the invading ureters and the "mature" tissue appearing at the core.

Some WTs are characterized by a histologic pattern where proliferation of undifferentiated metanephric blastemal cells is predominant [39] suggesting that errors in the second stage of nephrogenesis may be involved in Wilms tumorigenesis. In this context, the correlation between the underexpression of *WNT5A* and predominantly blastemal tumor histology could represent a cause for the absence of a secondary transition (i.e., mesenchymal-epithelial transition). However, given that WNT signaling pathway genes are affected by the promoter methylation status [40], *WNT5A* underexpression in WT samples could be the result of its promoter hypermethylation that hampers the normal transcription of the gene.

As a signal transducer, *WNT5A* might be suited for a key role in the complex cellular cross-talk between the developing ureter and the developing epithelia. Interestingly, up-regulation of *WNT5A* has previously been shown to suppress tubule branching during lung development [41]. *WNT5A* has also been implicated in regulating the mesenchymal-epithelial transition in uterine tissue [42].

In addition to its role in the regulation of branching morphogenesis [43,44], *PAX2* is also up-regulated during early kidney development and repressed in mature renal tissue [15,45]. Furthermore, *PAX2* is constitutively expressed in a variety of renal tumors including WT [45]. The *PAX2* knock down using specific siRNA and the WiT5A WT line showed a detectable level of *WNT5A* protein expression in samples treated with *PAX2*-siRNA$_1$ and *PAX2*-siRNA$_2$ (Figure 5, *B* and *D*). *WNT5A* expression increased slightly in both samples treated with *PAX2*-siRNA$_1$ and *PAX2*-siRNA$_2$ compared with nontreated samples (Figure 5, *A*, *B*, and *D*). Likewise, a detectable level of *PAX2* protein expression was detected in samples that had undergone *WNT5A*-siRNA$_2$ and *WNT5A*-siRNA$_6$ transfection (Figure 5, *C* and *E*). Based on this *in vitro* siRNA data, it is likely that when *PAX2* is highly expressed (i.e., in WT), the *WNT5A* is down-regulated (Figure 5*A*) and vice versa, although an *in vivo* study would be more suitable to confirm this hypothesis.

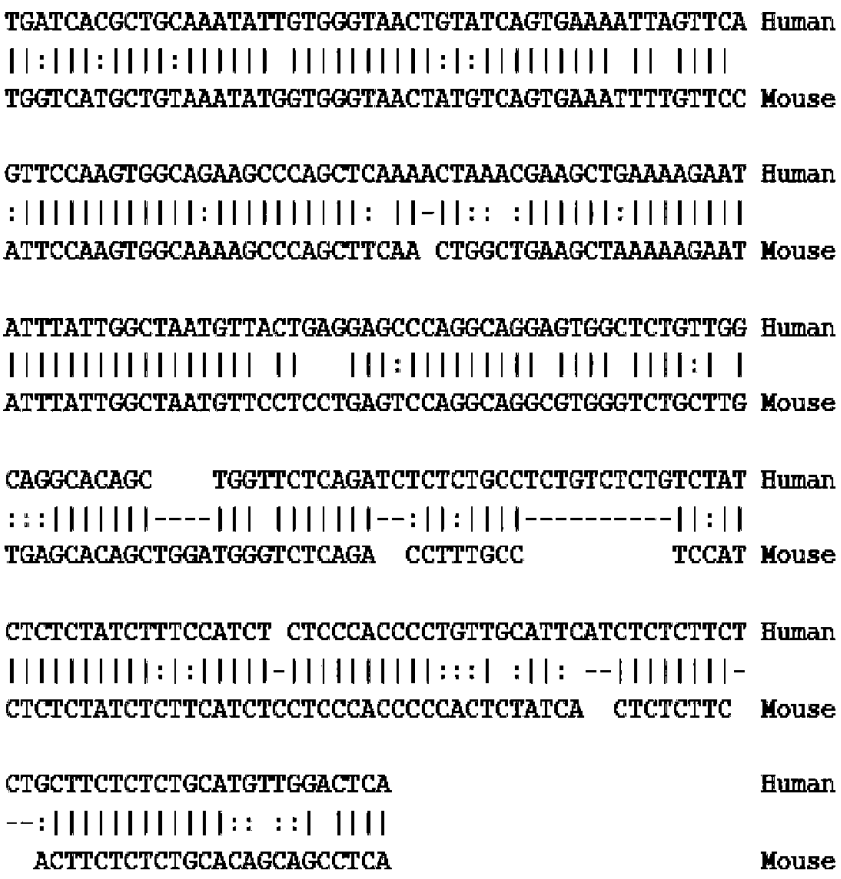

Figure 7. Alignment of the human ~300-bp *WNT5A*-responsive element with its counterpart in mouse 73% sequence identity. Human genomic upstream region of *WNT5A* was compared to the mouse counterpart and a percent identity plot (PIP) was generated. There are several regions of homologous sequence in the 100-kb 5′-upstream region. None of these homologous regions match known genes or expressed sequence tags and are therefore assumed to be noncoding regulatory sequences. The NACE-enriched ~300-bp fragment (bar) overlaps one of these homologous regions that share more than 70% identity with the mouse.

Reconciling these data with the expression analysis in Figure 6, it is tempting to speculate that *PAX2* and *WNT5A* share an inhibitory-like cross-relationship. *PAX2* tends to be overexpressed in Wilms tumors, whereas *WNT5A* tends to be underexpressed, and given that we now demonstrate that *PAX2* plays a specific regulatory role involving a *cis*-region of the *WNT5A* gene, an inhibitory relationship is entirely plausible.

During early renal development, up-regulated *PAX2* is suppressed by *WT1* after the completion of the first transitional stage [45], in more mature tissue, a dichotomy that is crucial to proper nephrogenesis [46]. *PAX2* inhibition of *WNT5A* would then be relieved, promoting the second transitional step. When *PAX2* is constitutively up-regulated, as it is in certain cases of WT, this second stage would not occur as reflected in the tumor histology (i.e., predominately blastemal).

A very recently discovered tumor suppressor gene *WTX*, operating through β-catenin, was shown to suppress the canonical WNT signaling pathway by enhancing β-catenin degradation [47]. Likewise, *WNT5A* was also shown to antagonize canonical Wnt/β-catenin signaling pathway [48] and regulate cell proliferation [49]. Given that both *WTX* and *WNT5A* genes block the Wnt/β-catenin signaling pathway, it is therefore likely that both genes operate through the same chain of command line [47,48]. This is the first report indicating a direct relationship between *PAX2* and *WNT5A* in the human embryonic kidney cells (HEK293) and indicating the importance of *PAX2* in the regulation of this transcription factor and member of the WNT pathway. Further study is necessary to identify other intermediary molecules involved in these pathways and to determine whether the *PAX2* and *WNT5A* are truly involved in WT pathogenesis.

Acknowledgments

The authors thank Elizabeth Perlman for review and classification of tumors' histology and Weizheng Guo and Ana Milanovic for their technical support.

References

[1] Beckwith JB (1998). National Wilms Tumor Study: an update for pathologists. *Pediatr Dev Pathol* **1** (1), 79–84.
[2] Beckwith JB, Kiviat NB, and Bonadio JF (1990). Nephrogenic rests, nephroblastomatosis, and the pathogenesis of Wilms' tumor. *Pediatr Pathol* **10** (1–2), 1–36.
[3] Charles AK, Brown KW, and Berry PJ (1998). Microdissecting the genetic events in nephrogenic rests and Wilms' tumor development. *Am J Pathol* **153** (3), 991–1000.
[4] Park S, Bernard A, Bove KE, Sens DA, Hazen-Martin DJ, Garvin AJ, and Haber DA (1993). Inactivation of WT1 in nephrogenic rests, genetic precursors to Wilms' tumour. *Nat Genet* **5** (4), 363–367.
[5] Van Heyningen V and Hastie ND (1992). Wilms' tumour: reconciling genetics and biology. *Trends Genet* **8** (1), 16–21.
[6] Call KM, Glaser T, Ito CY, Buckler AJ, Pelletier J, Haber DA, Rose EA, Kral A, Yeger H, Lewis WH, et al. (1990). Isolation and characterization of a zinc finger polypeptide gene at the human chromosome 11 Wilms' tumor locus. *Cell* **60** (3), 509–520.

[7] Dahl E, Koseki H, and Balling R (1997). Pax genes and organogenesis. *Bioessays* **19** (9), 755–765.

[8] Haber DA, Buckler AJ, Glaser T, Call KM, Pelletier J, Sohn RL, Douglass EC, and Housman DE (1990). An internal deletion within an 11p13 zinc finger gene contributes to the development of Wilms' tumor. *Cell* **61** (7), 1257–1269.

[9] Huang A, Campbell CE, Bonetta L, McAndrews-Hill MS, Chilton-MacNeill S, Coppes MJ, Law DJ, Feinberg AP, Yeger H, and Williams BR (1990). Tissue, developmental, and tumor-specific expression of divergent transcripts in Wilms tumor. *Science* **250** (4983), 991–994.

[10] Treisman J, Harris E, and Desplan C (1991). The paired box encodes a second DNA-binding domain in the paired homeo domain protein. *Genes Dev* **5** (4), 594–604.

[11] Brophy PD, Ostrom L, Lang KM, and Dressler GR (2001). Regulation of ureteric bud outgrowth by Pax2-dependent activation of the glial derived neurotrophic factor gene. *Development* **128** (23), 4747–4756.

[12] Dressler GR, Wilkinson JE, Rothenpieler UW, Patterson LT, Williams-Simons L, and Westphal H (1993). Deregulation of Pax-2 expression in transgenic mice generates severe kidney abnormalities. *Nature* **362** (6415), 65–67.

[13] Torres M, Gomez-Pardo E, Dressler GR, and Gruss P (1995). Pax-2 controls multiple steps of urogenital development. *Development* **121** (12), 4057–4065.

[14] Torres M, Gomez-Pardo E, and Gruss P (1996). Pax2 contributes to inner ear patterning and optic nerve trajectory. *Development* **122** (11), 3381–3391.

[15] Dressler GR (1996). Pax-2, kidney development, and oncogenesis. *Med Pediatr Oncol* **27** (5), 440–444.

[16] Dressler GR and Douglass EC (1992). Pax-2 is a DNA-binding protein expressed in embryonic kidney and Wilms tumor. *Proc Natl Acad Sci USA* **89** (4), 1179–1183.

[17] Eccles MR, Yun K, Reeve AE, and Fidler AE (1995). Comparative *in situ* hybridization analysis of *PAX2*, *PAX8*, and *WT1* gene transcription in human fetal kidney and Wilms' tumors. *Am J Pathol* **146** (1), 40–45.

[18] Dziarmaga A, Hueber PA, Iglesias D, Hache N, Jeffs A, Gendron N, Mackenzie A, Eccles M, and Goodyer P (2006). Neuronal apoptosis inhibitory protein (NAIP) is expressed in developing kidney and is regulated by *PAX2*. *Am J Physiol Renal Physiol* **291** (4), F913–F920.

[19] Porteous S, Torban E, Cho NP, Cunliffe H, Chua L, McNoe L, Ward T, Souza C, Gus P, Giugliani R, et al. (2000). Primary renal hypoplasia in humans and mice with *PAX2* mutations: evidence of increased apoptosis in fetal kidneys of *Pax2(1Neu)*$^{+/-}$ mutant mice. *Hum Mol Genet* **9** (1), 1–11.

[20] Sanyanusin P, McNoe LA, Sullivan MJ, Weaver RG, and Eccles MR (1995). Mutation of *PAX2* in two siblings with renal-coloboma syndrome. *Hum Mol Genet* **4** (11), 2183–2184.

[21] Sanyanusin P, Schimmenti LA, McNoe LA, Ward TA, Pierpont ME, Sullivan MJ, Dobyns WB, and Eccles MR (1995). Mutation of the *PAX2* gene in a family with optic nerve colobomas, renal anomalies and vesicoureteral reflux. *Nat Genet* **9** (4), 358–364.

[22] Torban E, Eccles MR, Favor J, and Goodyer PR (2000). *PAX2* suppresses apoptosis in renal collecting duct cells. *Am J Pathol* **157** (3), 833–842.

[23] Dziarmaga A, Clark P, Stayner C, Julien JP, Torban E, Goodyer P, and Eccles M (2003). Ureteric bud apoptosis and renal hypoplasia in transgenic *PAX2-Bax* fetal mice mimics the renal-coloboma syndrome. *J Am Soc Nephrol* **14** (11), 2767–2774.

[24] Clark P, Dziarmaga A, Eccles M, and Goodyer P (2004). Rescue of defective branching nephrogenesis in renal-coloboma syndrome by the caspase inhibitor, Z-VAD-fmk. *J Am Soc Nephrol* **15** (2), 299–305.

[25] Tamimi Y, Dietrich K, Stone K, and Grundy P (2006). Paired box genes, *PAX-2* and *PAX-8*, are not frequently mutated in Wilms tumor. *Mutat Res* **601** (1–2), 46–50.

[26] Tamimi Y, Lines M, Coca-Prados M, and Walter MA (2004). Identification of target genes regulated by FOXC1 using nickel agarose–based chromatin enrichment. *Invest Ophthalmol Vis Sci* **45** (11), 3904–3913.

[27] Weinmann AS and Farnham PJ (2002). Identification of unknown target genes of human transcription factors using chromatin immunoprecipitation. *Methods* **26** (1), 37–47.

[28] Weinmann AS, Yan PS, Oberley MJ, Huang TH, and Farnham PJ (2002). Isolating human transcription factor targets by coupling chromatin immunoprecipitation and CpG island microarray analysis. *Genes Dev* **16** (2), 235–244.

[29] Phelps DE and Dressler GR (1996). Identification of novel Pax-2 binding sites by chromatin precipitation. *J Biol Chem* **271** (14), 7978–7985.

[30] Birney E, Andrews D, Bevan P, Caccamo M, Cameron G, Chen Y, Clarke L, Coates G, Cox T, Cuff J, et al. (2004). Ensembl 2004. *Nucleic Acids Res* **32** (Database issue), D468–D470.

[31] Grundy PE, Breslow NE, Li S, Perlman E, Beckwith JB, Ritchey ML, Shamberger RC, Haase GM, D'Angio GJ, Donaldson M, et al. (2005). Loss of heterozygosity for chromosomes 1p and 16q is an adverse prognostic factor in favorable-histology Wilms tumor: a report from the National Wilms Tumor Study Group. *J Clin Oncol* **23** (29), 7312–7321.

[32] Winer J, Jung CK, Shackel I, and Williams PM (1999). Development and validation of real-time quantitative reverse transcriptase–polymerase chain reaction for monitoring gene expression in cardiac myocytes *in vitro*. *Anal Biochem* **270** (1), 41–49.

[33] Dressler GR (2006). The cellular basis of kidney development. *Annu Rev Cell Dev Biol* **22**, 509–529.

[34] Sredni ST, de Camargo B, Lopes LF, Teixeira R, and Simpson A (2001). Immunohistochemical detection of p53 protein expression as a prognostic indicator in Wilms tumor. *Med Pediatr Oncol* **37** (5), 455–458.

[35] Szuhai K, Ijszenga M, Tanke HJ, Rosenberg C, and Hogendoom PC (2006). Molecular cytogenetic characterization of four previously established and two newly established Ewing sarcoma cell lines. *Cancer Genet Cytogenet* **166** (2), 173–179.

[36] Saitoh T and Katoh M (2002). Expression and regulation of *WNT5A* and *WNT5B* in human cancer: up-regulation of *WNT5A* by TNFalpha in MKN45 cells and up-regulation of *WNT5B* by beta-estradiol in MCF-7 cells. *Int J Mol Med* **10** (3), 345–349.

[37] Park S, Schalling M, Bernard A, Maheswaran S, Shipley GC, Roberts D, Fletcher J, Shipman R, Rheinwald J, Demetri G, et al. (1993). The Wilms tumour gene *WT1* is expressed in murine mesoderm–derived tissues and mutated in a human mesothelioma. *Nat Genet* **4** (4), 415–420.

[38] Barasch J, Pressler L, Connor J, and Malik A (1996). A ureteric bud cell line induces nephrogenesis in two steps by two distinct signals. *Am J Physiol* **271** (1 Pt 2), F50–F61.

[39] Hastie ND (1994). The genetics of Wilms' tumor—a case of disrupted development. *Annu Rev Genet* **28**, 523–558.

[40] Martin V, Agirre X, Jimenez-Velasco A, Jose-Eneriz ES, Cordeu L, Garate L, Vilas-Zornoza A, Castillejo JA, Heiniger A, Prosper F, et al. (2008). Methylation status of Wnt signaling pathway genes affects the clinical outcome of Philadelphia-positive acute lymphoblastic leukemia. *Cancer Sci* **99**, 1865–1868.

[41] Li C, Hu L, Xiao J, Chen H, Li JT, Bellusci S, Delanghe S, and Minoo P (2005). Wnt5a regulates Shh and Fgf10 signaling during lung development. *Dev Biol* **287** (1), 86–97.

[42] Mericskay M, Kitajewski J, and Sassoon D (2004). Wnt5a is required for proper epithelial-mesenchymal interactions in the uterus. *Development* **131** (9), 2061–2072.

[43] Grote D, Souabni A, Busslinger M, and Bouchard M (2006). *Pax2/8*–regulated Gata3 expression is necessary for morphogenesis and guidance of the nephric duct in the developing kidney. *Development* **133** (1), 53–61.

[44] Narlis M, Grote D, Gaitan Y, Boualia SK, and Bouchard M (2007). *Pax2* and *pax8* regulate branching morphogenesis and nephron differentiation in the developing kidney. *J Am Soc Nephrol* **18** (4), 1121–1129.

[45] Ryan G, Steele-Perkins V, Morris JF, Rauscher FJ, and Dressler GR (1995). Repression of *Pax-2* by *WT1* during normal kidney development. *Development* **121** (3), 867–875.

[46] Beland M and Bouchard M (2006). *PAX* gene function during kidney tumorigenesis: a comparative approach. *Bull Cancer* **93** (9), 875–882.

[47] Major MB, Camp ND, Berndt JD, Yi X, Goldenberg SJ, Hubbert C, Biechele TL, Gingras AC, Zheng N, and Maccoss MJ (2007). Wilms tumor suppressor WTX negatively regulates WNT/beta-catenin signaling. *Science* **316** (5827), 1043–1046.

[48] Ishitani T, Kishida S, Hyodo-Miura J, Ueno N, Yasuda J, Waterman M, Shibuya H, Moon RT, Ninomiya-Tsuji J, and Matsumoto K (2003). The TAK1-NLK mitogen-activated protein kinase cascade functions in the Wnt-5a/Ca(2+) pathway to antagonize Wnt/beta-catenin signaling. *Mol Cell Biol* **23** (1), 131–139.

[49] Yamaguchi TP, Bradley A, McMahon AP, and Jones S (1999). A Wnt5a pathway underlies outgrowth of multiple structures in the vertebrate embryo. *Development* **126** (6), 1211–1223.